



# An isothermal decomposition dynamics research instrument and its application in HMX/TNT/Al composite explosive

Liqiong Luo<sup>1</sup> · Penglin Guo<sup>2</sup> · Bo Jin<sup>1</sup> · Yiyi Xiao<sup>1</sup> · Qingchun Zhang<sup>1</sup> · Shijin Chu<sup>1</sup> · Rufang Peng<sup>1</sup>

Received: 11 January 2019 / Accepted: 2 July 2019 / Published online: 1 August 2019  
© Akadémiai Kiadó, Budapest, Hungary 2019

## Abstract

An isothermal decomposition dynamics research instrument that uses a pressure sensor with the ability to withstand high temperatures for investigating sublimated samples was established. The isothermal decomposition of HMX/TNT/Al (HTA) composite explosive was investigated by this instrument, and the corresponding thermal decomposition kinetic parameters were obtained with the method of isothermal decomposition dynamics research. Arrhenius equation and model-fitting method were used to calculate the thermal decomposition kinetic parameters based on the experimental data obtained by the improved instrument. Results of the Arrhenius equation and model-fitting method were consistent with an average  $E_a$  of  $146.56 \text{ kJ mol}^{-1}$  and  $\ln A$  of  $13.29 \text{ s}^{-1}$ . The model-fitting method further proved that the mechanism of thermal decomposition of HTA composite explosive was controlled by 3D diffusion. The instrument was also used to predict the storage life of HTA. Results showed that the effective storage life of HTA at ambient temperature ( $25 \text{ }^\circ\text{C}$ ) is 229 years, whereas the extent of reaction reached 0.5%.

**Keywords** Energetic materials · Instrument improvement · Isothermal decomposition dynamics · Storage life

## Introduction

The thermal decomposition of explosives is closely related to temperature. Generally, the reaction rate of the thermal decomposition of explosive increases with increased temperature, thereby releasing considerable amounts of gas and heat that lead to autocatalytic behaviour and even cause explosion events. Hence, the thermal stability, reaction mechanism, and kinetics of thermal decomposition are important indicators for explosives, which help in evaluating their practical safety and storage.

At present, various methods, including differential scanning calorimetry, thermogravimetry, Fourier transform

infrared spectroscopy, and accelerating rate calorimetry, have been applied to investigate the thermal decomposition of explosive [1–7]. Their determinations are based on quality or energy changes. In addition, gas manometric techniques have also generated considerable interest in determining the thermal stability of explosives. Due to convenient operation of vacuum stability test, it is widely used to measure the thermal decomposition of many chemicals including explosives [8–11]. However, a mercury manometer is a potential threat if its pipe was broken [12, 13]. A Bourdon pressure gauge, which is based on the indirect pressure measurement principle, cannot monitor the reaction process continuously [14, 15]. The modified Czechoslovak manometric method (STABIL method) is able to automatically monitor pressure variables but cannot show temperature change [7, 16]. The dynamic vacuum stability test method (DVST) monitors the reaction process continuously and directly [3, 17–19]. The orifice of test tube is sealed by perfect vacuum silicon fat and glass cock; thus, the month-long test cannot be carried out by the instrument.

Early, we had established a new isothermal decomposition dynamics research instrument to solve these

✉ Bo Jin  
jinbo0428@163.com

✉ Rufang Peng  
rfpeng2006@163.com

<sup>1</sup> State Key Laboratory of Environmental Friendly Energy Materials, Southwest University of Science and Technology, Mianyang 621010, Sichuan, China

<sup>2</sup> Institution of Chemical Materials, China Academy of Engineering Physics, Mianyang 621010, China

problems and used this method to study the isothermal decomposition kinetics of CL-20 and nitrocellulose [20, 21]. However, the previous instrument cannot be used for sublimation samples, such as 2,4,6-trinitrotoluene (TNT) and TNT-based composite explosives. In this work, the isothermal decomposition dynamics research instrument was further improved and the isothermal decomposition kinetics of HTA composite explosive was successfully studied using this improved instrument. Compared with the above-mentioned thermal analysis methods, the instrument is able to monitor the reaction process continuously for several months and predict the storage life.

## Experimental

### Materials

HTA composite explosive, which is composed of  $\beta$ -octahydro-1,3,5,7-tetranitro-1,3,5,7-tetrazocine ( $\beta$ -HMX, 55%), 2,4,6-trinitrotoluene (TNT, 30%), aluminium powder (Al, 8%), and other reagents (7%), was supplied by the China Academy of Engineering Physics (Mianyang, Sichuan). Before the test, the sample was sieved to the average particle size (200–300 mesh) by the sieve and freeze-dried. To avoid the effects of adsorbed gaseous impurities on the composite explosive, it was stored in a vacuum desiccator containing silica gel desiccant prior to testing.

### Apparatus and conditions

Analysis was performed using elite high-performance liquid chromatography (HPLC) P230. The separation was done on a UV detector, and sampling was performed by autosampler. Data collection for chromatogram was done by N2000. The column was Welchrom-C18 (250  $\times$  4.6 mm) with mobile phase of methanol. Filtration of mobile phase was carried out by 0.45- $\mu$ m membrane filter under the isocratic condition with a flow rate of 0.5 mL min<sup>-1</sup>, injected volume was 20  $\mu$ L, and elution was monitored at 249 nm with run time of 20 min.

The improved instrument is composed of a temperature sensor, pressure sensor, stainless-steel test tube with gold-plated walls, thermostat, vacuum pump, pressure transmitter, DC power supply, and computer. Figure 1 shows the detailed components. The pressure sensors were connected with DC power supply, and the values recorded by pressure sensors were sent to an acquisition–processing unit. The measuring range of the pressure sensor is 0–100 kPa or 0–200 kPa with the accuracy of 0.25% over 250 °C. Thermal reaction units were sealed tightly and

evacuated to the initial pressure below 0.1 kPa, and pressure values remain stable without fluctuation for over 7 days to ensure well sealing (Fig. 2). After setting the heating program of temperature controller, the reaction units were heated from room temperature to the target temperature with a constant heating rate and then maintained at the target temperature isothermally unremittingly. The reaction units were connected to data acquisition–processing units and placed into the thermostat, and data collection interval was set to 1 min. Samples were studied isothermally at different temperatures (110 °C, 120 °C, 130 °C, 140 °C, and 150 °C). Fifty milligrams of samples was added to the test tube with 5 mL volume and 1.45-mm wall thickness. To calculate the total free gas of 50 mg HTA, 15 mg HTA was investigated at 230 °C. Before the test, the test tube must be washed with acetone and ethanol and then dried to guarantee that the instrument was clean and the result was credible.

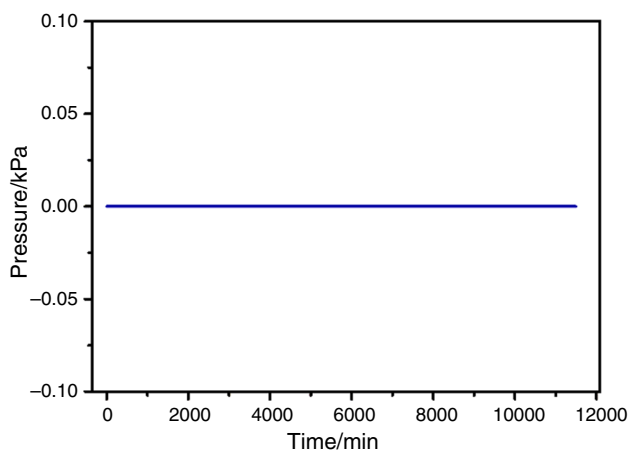
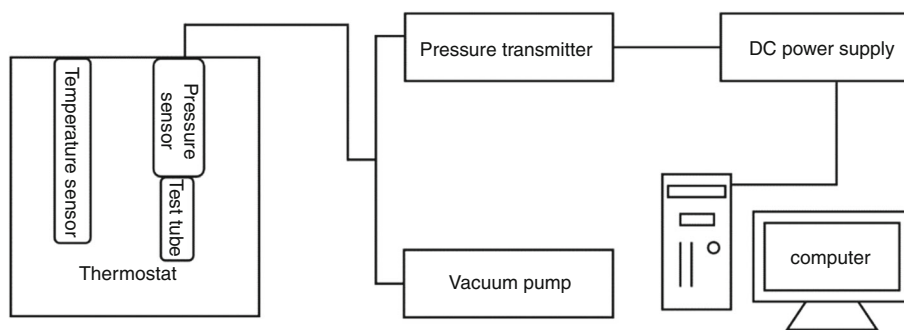
## Results and discussion

### Instrument improvement

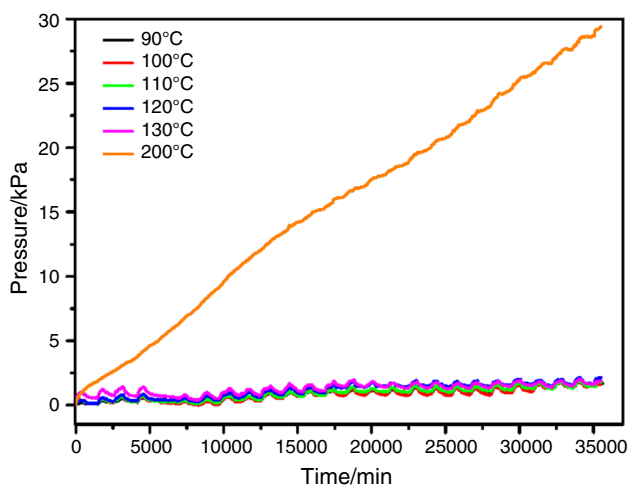
Originally, the experiment on the isothermal decomposition of HTA composite explosive was performed via our previously reported isothermal decomposition dynamics research instrument [20] at different temperatures (90 °C, 100 °C, 110 °C, 120 °C, 130 °C, and 200 °C). Figure 3 presents variation of gas pressure with time, indicating that the relationship between temperature and pressure is not regular. We speculate that this phenomenon is due to the sublimation of TNT in HTA. The pressure sensor and test sample are in different temperature fields because the pressure sensor used in this instrument does not withstand high temperatures. Thus, the TNT component in the test sample is heated, sublimated, and eventually condensed in the top of test tube and connector when the temperature is below 60 °C. As we predicted, a canary yellow crystal was discovered at the connector when the reaction unit was disassembled as shown in Fig. 4. To further confirm the canary yellow crystal, analysis by HPLC indicates that it is exactly TNT as shown in Fig. 5. Thus, our previously reported isothermal decomposition dynamics research instrument cannot be applied to the samples with the sublimation components. To overcome this problem, we further improved the isothermal decomposition dynamics research instrument.

Figure 6 demonstrates the improved isothermal decomposition dynamics research instrument. Improvements have been added to the instrument in comparison with the previous instrument [20]. First, the heat-sensing pressure sensor was replaced with a heat-resistant pressure

**Fig. 1** Schematic of components connecting the improved isothermal decomposition dynamics research instrument



**Fig. 2** Curve of time dependence of pressure during sealing test via the improved instrument



**Fig. 3** Time dependence of gas pressure of HTA at different temperatures via our previously reported isothermal decomposition dynamics research instrument

sensor whose pressure switch element is sapphire. Sapphire is selected due to single crystal and insulator elements so that excellent elasticity and insulation characteristics are achieved rather than hysteresis, fatigue, and creep. Second, the sensor was separated from the pressure transmitter so

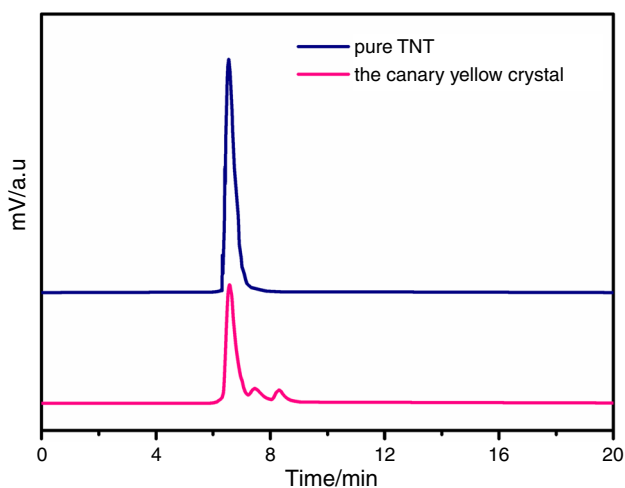
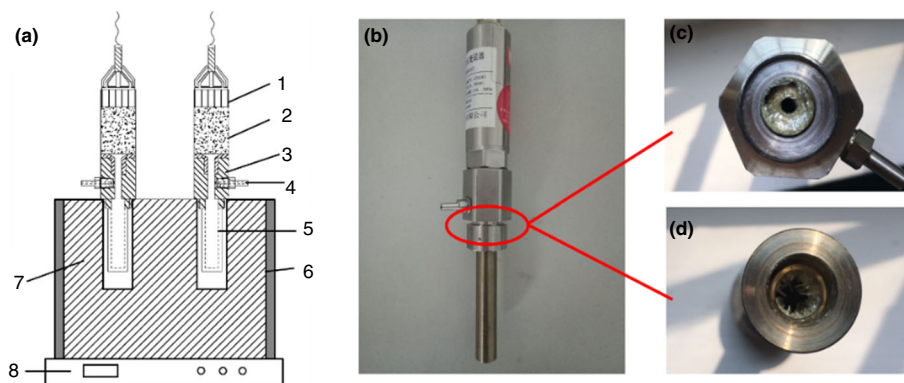
that the pressure sensor is not affected by room temperature. The vacuum valve where thermal reaction units were sealed tightly by the soft metal gasket was the self-developed mini-valve instead of the traditional vacuum valve. The structure of the self-developed mini-valve is shown in Fig. 7. The hole is on the side instead of bottom to prevent from being blocked by soft metal. And the thermal reaction units including the pressure sensors, connectors and test tubes were placed in the same temperature environment to avoid the influence from coagulation of explosives. Moreover, the thermostat was also improved. In consideration of security, the thermostat of the instrument was cast aluminium instead of oil bath. The temperature controller adopts a fully automatic control system running automatically from room temperature to the set temperature after setting a program with a function of over-temperature alarm and variability from 0 °C to 300 °C with an accuracy of  $\pm 0.5$  °C. In addition, each instrument has four reaction chambers that can measure four samples at one time.

### Thermal stability

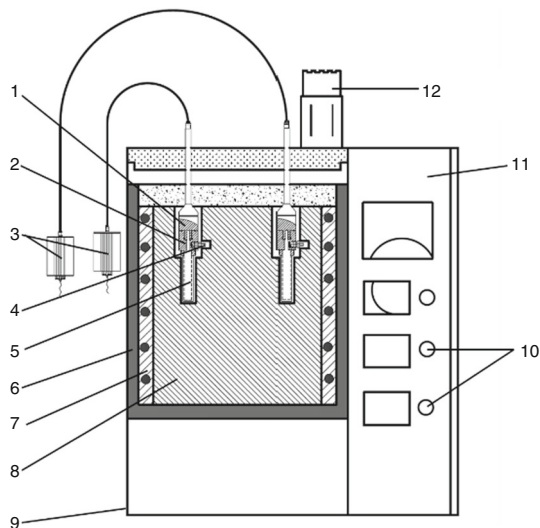
The sample was measured isothermally via the instrument at temperatures of 110 °C, 120 °C, 130 °C, 140 °C, 150 °C, and 230 °C. During the entire reaction process, the gas pressure generated by the decomposition of the measurement sample is automatically collected and recorded at regular intervals. The Clausius–Clapeyron equation of TNT is  $\ln P = 31.00 - 10,722.39/T$  through consulting literature materials [22], where  $P$  (Pa) is the saturation vapour pressure of TNT, and  $T$  is the temperature (K). According to the equation, the saturation vapour pressure at different temperatures was obtained and is listed in Table 1. And then, the pressure obtained by the instrument deducted the value of saturation vapour pressure of TNT at the corresponding temperature. The pressure values were converted into standard values under unified temperature of 25 °C in accordance with the following equation:

$$PV = nRT \quad (1)$$

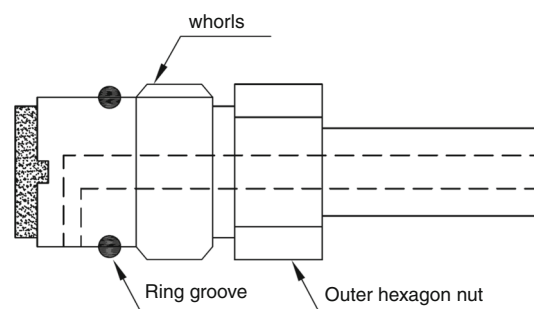
**Fig. 4** **a** Schematic of our previously reported isothermal decomposition dynamics research instrument: 1—pressure transmitter, 2—pressure sensor, 3—connector, 4—mini-valve, 5—test tube, 6—insulating jacket, 7—heater, 8—temperature controller. **b** Photograph of thermal reaction and the distribution of the canary yellow crystal; **c** connector; **d** test tube



**Fig. 5** HPLC chromatograms of pure TNT and the canary yellow crystal at the connector



**Fig. 6** Schematic of the improved instrument: 1—pressure sensor, 2—connector, 3—pressure transmitter, 4—mini-valve, 5—test tube, 6—insulating jacket, 7—cast aluminium, 8—soaking zone, 9—body, 10—temperature controller, 11—electricity box, 12—shelf for test tube



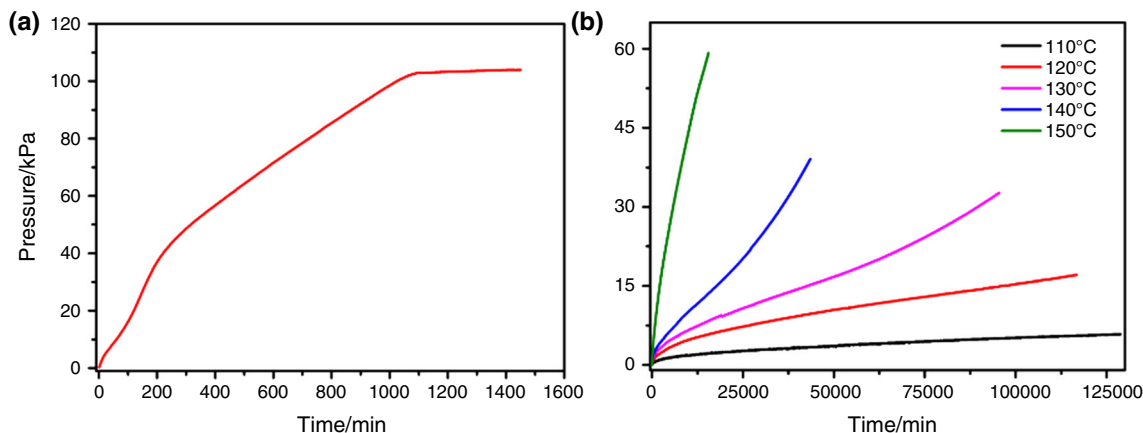
**Fig. 7** Structure of mini-valve

Figure 8 presents the time dependence of the standardized gas pressure of HTA under the unified temperature. The process of thermal decomposition at 230 °C from the acceleration period to the constant velocity and deceleration period is clearly illustrated (Fig. 8a). The sample gradually starts decomposing, and the pressure in the reactor system gradually increases over time until it is constant. At 230 °C, the time observed to complete the conversion of 15 mg HTA is 1102 min, and the total gas pressure is 103.94 kPa. The result indicates that the gas pressure produced by the complete decomposition of 50 mg samples is 346.47 kPa.

The gas pressure significantly increases with the increase in temperature, which suggests that the storage temperature has a significant influence on the stability and storage life of HTA (Fig. 8b). At low temperature (110 °C), the thermal decomposition process of HTA presents a slow reaction rate stage, which is not significant under high temperatures. Thus, the reaction constant rate increases with increasing temperature. To discuss the results deeply, the kinetic parameters were calculated by Arrhenius equation and model-fitting method.

**Table 1** Saturation vapour pressure of TNT at different temperatures

Temperature/°C	110	120	130	140	150	230
Saturation vapour pressure/kPa	0.02	0.04	0.08	0.16	0.29	16.15



**Fig. 8** Time dependence of the standardized gas pressure of HTA under the unified temperature of 25 °C: **a** complete decomposition at 230 °C; **b** at different temperatures of 110 °C, 120 °C, 130 °C, 140 °C, and 150 °C

**Kinetics**

The thermal decomposition kinetics of explosives partly reflects its reaction rate constant and thermal stability. The extent of reaction at any time ( $\alpha$ ) [20] is as follows:

$$\alpha = \frac{P}{P_T} \tag{2}$$

where  $P$  (kPa) is the standard pressure of gas at any time and  $P_T$  (kPa) denotes total gas pressure produced by complete decomposition.

The complete decomposition pressure of the 50 mg sample would produce 346.47 kPa of gas, so the pressure is

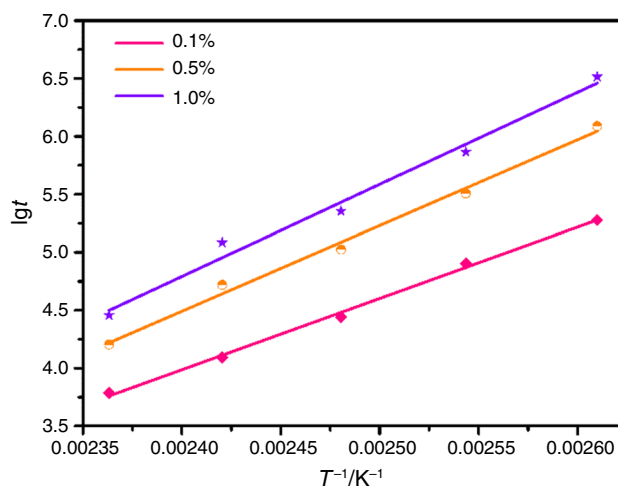


**Fig. 9** Plot of  $\lg \alpha$  versus  $T^{-1}$  of HTA

**Table 2** Time of HTA to attain a certain extent of reaction at different temperatures

Extent of reaction/ $\alpha$	Time/min				
	110 °C	120 °C	130 °C	140 °C	150 °C
0.1%	120	55	42	20	14
0.2%	347	212	102	50	30
0.3%	852	439	190	88	50
0.4%	1724	805	303	140	75
0.5%	3159	1338	459	207	102
1.0%	20,465	5359	1764	876	267
1.5%	54,605	12,219	3765	2027	478

**Table 3** Kinetic parameters of HTA to reach various extents based on Arrhenius equation

Extent of reaction/ $\alpha$	$E_a$ /kJ mol <sup>-1</sup>	$\lg A$	R
0.5%	117.86	10.79	0.9963
1.0%	141.60	13.26	0.9909
1.5%	152.14	14.28	0.9822

**Table 4** Decomposition reaction constant rate and mechanism function of HTA via model-fitting method

Temperature/°C	Model no.	Model name	$k \times 10^{-11}/s^{-1}$	$G(\alpha)$
110	9	Z-L-T equation	1.45	$[(1 - \alpha)^{1/3} - 1]^2$
120	9	Z-L-T equation	3.51	$[(1 - \alpha)^{1/3} - 1]^2$
130	8	Anti-Jander equation	10.73	$[(1 + \alpha)^{1/3} - 1]^2$
140	8	Anti-Jander equation	24.00	$[(1 + \alpha)^{1/3} - 1]^2$
150	8	Anti-Jander equation	50.58	$[(1 + \alpha)^{1/3} - 1]^2$

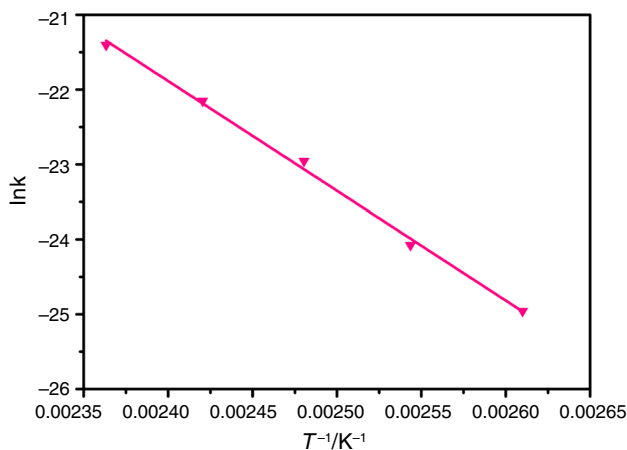


**Fig. 10** Plot of  $\ln k$  against  $T^{-1}$  of HTA

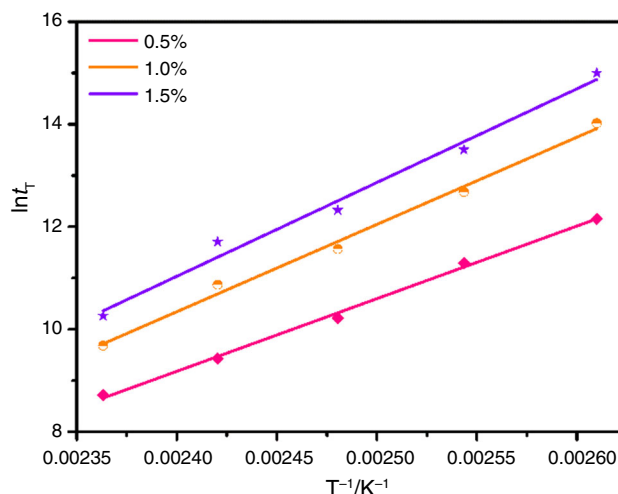


**Fig. 12** Plot of  $\ln t_T$  against  $T^{-1}$  of HTA

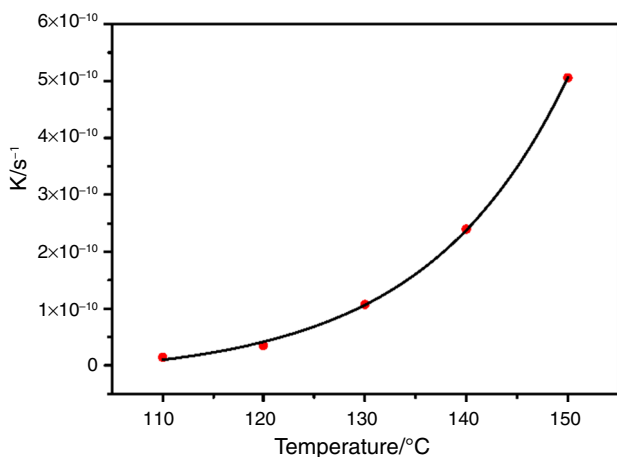


**Fig. 11** Curve of  $k$  against temperature

3.46 kPa when the extent of reaction achieved 1.0% and above. Table 2 presents the time of HTA to attain a certain extent of reaction at different temperatures. Time ranged from 267 min to 20,465 min, which exceed 77 times between 150 and 110 °C when the conversion fraction was 1.0%.

The data of Table 2 were calculated by Arrhenius equation [23]:

$$\lg t = -\lg A + E_a/2.303RT \tag{3}$$

where  $t$  is the time required to attain a certain extent of reaction (s),  $A$  denotes the pre-exponential factor( $s^{-1}$ ),  $E_a$  represents the activation energy ( $\text{kJ mol}^{-1}$ ),  $R$  stands for the gas constant ( $8.314 \text{ kJ K}^{-1} \text{ mol}^{-1}$ ), and  $T$  indicates the temperature (K). Figure 9 shows that the apparent activation energy  $E_a$  and the pre-exponential factor  $A$  are obtained from the slope of the line (Table 3).

The data of isothermal decomposition were also reckoned in accordance with the solid-phase reaction equation by using model-fitting method [24, 25], namely solid-phase decomposition reaction kinetics equation:

$$G(\alpha) = kt \tag{4}$$

where  $G(\alpha)$  is the integral form of the mechanism function,  $\alpha$  denotes the conversion rate,  $k$  represents the reaction rate constant, and  $t$  refers to the reaction time. The model-fitting method for isothermal kinetic is reliable because temperature is held constant during each experiment [24]. For a one-order reaction, the reaction rate constant  $k$  is separated



**Table 5** Empirical formulas and estimated time to reach a certain extent at various temperatures based on Semenov's equation

Extent of reaction ( $\alpha$ )	Empirical formulas	$R$		Time	Time	Time	Time
				25 °C	30 °C	70 °C	110 °C
0.5%	$\ln t_T = 14,173.48/T - 24.84$	0.9963	Calculated value	229 years	105 years	164 days	3167 min
			Measured value	–	–	–	3159 min
1.0%	$\ln t_T = 17,028.02/T - 30.52$	0.9909	Calculated value	11,166 years	4353 years	6 years	18,451 min
			Measured value	–	–	–	20,465 min
1.5%	$\ln t_T = 18,295.88/T - 32.88$	0.9822	Calculated value	74,706 years	27,152 years	24 years	48,058 min
			Measured value	–	–	–	54,605 min

with the reaction model  $G(\alpha)$ . The fitting line of  $G(\alpha)$  versus  $t$  passes the origin of coordinates. The isothermal kinetics processing software presents 41 types of lines of  $G(\alpha)$  versus  $t$  by using least-squares method. The most proper form of  $G(\alpha)$  is selected on the basis of the fitting line with the maximum correlation coefficient and the minimum intercept [26]. The reaction rate constant  $k$  is obtained by the slope. Through the  $G(\alpha)$  versus  $t$  relationship of linear regression for the extent of reaction (0.1%, 0.2%, 0.3%, 0.4%, 0.5%), best mechanism functions and kinetics parameters under different temperatures were obtained (Table 4). Then, the Arrhenius parameters were evaluated via the Arrhenius equation:

$$\ln k = -E_a/RT + \ln A \quad (5)$$

where  $k$  is the reaction rate constant ( $s^{-1}$ ),  $E_a$  represents the activation energy ( $kJ mol^{-1}$ ),  $R$  denotes the gas constant ( $8.314 kJ K^{-1} mol^{-1}$ ),  $T$  indicates the temperature (K), and  $A$  refers to the pre-exponential factor ( $s^{-1}$ ).

For HTA, at 110 °C–120 °C, the models conformed to the Z–L–T equation [26] described as 3D diffusion, whereas at 130 °C–150 °C, the models are the Anti-Jander equation with 3D diffusion. When  $\ln k$  is plotted against  $T^{-1}$ , a straight line is obtained through linear fitting (Fig. 10), and the experimental points are described as  $\ln k = -14,656.51/T + 13.29$  with  $R = 0.9961$ . The average  $E_a$  is  $146.56 kJ mol^{-1}$  with  $\ln A$  13.29 in accordance with the Arrhenius equation. Evidently, the  $k$  value exhibits a strong relationship to temperature. The dependence of reaction rate on temperature is the exponential growth trend as shown in Fig. 11.

### Storage life

The total gas amount of complete thermal decomposition was used to determine the extent of reaction in accordance with Eq. (2). The end point of the life corresponds to the extents of reaction of 0.5%, 1.0%, and 1.5%. The storage life of HTA at 25 °C, 30 °C, 70 °C, and 110 °C was estimated using Semenov's equation [26] as follows:

$$\ln t_T = a + b/T \quad (6)$$

where  $t_T$  is the reaction time to reach a certain extent of reaction,  $a$  and  $b$  denote the undetermined coefficients, and  $T$  indicates the temperature (K). In accordance with the fitting line of Semenov's equation, the coefficients  $a$  and  $b$  are determined and the storage life at ambient temperature is the correct inference. Figure 12 shows that the plots of  $\ln t_T$  against  $T^{-1}$  are fitting. Table 5 exhibits the empirical formulas and the storage life corresponding to a certain extent of reaction at different temperatures. At 110 °C, the storage life values of HTA are 3167, 18,451, and 48,058 min with the extents of reaction of 0.5%, 1.0%, and 1.5%, respectively. The results are consistent with the experimental measured values. The effective storage life of HTA at ambient temperature (25 °C) is 229 years when the extent of reaction reached 0.5%.

### Conclusions

The isothermal decomposition dynamics research instrument was improved further. Monitoring of the reaction process continuously was achieved by the dynamic monitoring pressure sensor combined with a data acquisition–processing unit. The effect to the coagulation of explosives and the effect of the temperature were overcome. In addition, the thermal decomposition of HTA composite explosive was investigated using the improved instrument. Arrhenius equation and model-fitting method have been applied to determine the thermal decomposition kinetics of HTA with an average  $E_a$  of  $146.56 kJ mol^{-1}$  and  $\ln A$  of  $13.29 s^{-1}$ . The mechanism of the thermal decomposition of HTA composite explosive is controlled by 3D diffusion. Additionally, the effective storage life of HTA at ambient temperature (25 °C) is 229 years ( $\alpha = 0.5\%$ ). Overall, the instrument avoided the effects of coagulation and temperature.

**Acknowledgements** We are grateful for financial support from the Science Challenge Project (Project No. TZ2018004), the Natural

Science Foundation of China (21,875,192, 11602240), National Defense Technology Foundation Project (Project No. JSJL2016404B002), Key Projects of the Pre-research Fund of the General Armament Department (Project No. 6140720020101), and China Academy of Engineering Physics Research Institute (18zh0080).

## References

- Rothgery EF, Audette DE, Wedlich RC, Csejka DA. The study of the thermal decomposition of 3-nitro-1,2,4-triazol-5-one (NTO) by DSC, TGA-MS, and ARC. *Thermochim Acta*. 1991;185:235–43.
- Sinapour H, Damiri S, Pouretedal HR. The study of RDX impurity and wax effects on the thermal decomposition kinetics of HMX explosive using DSC/TG and accelerated aging methods. *J Therm Anal Calorim*. 2017;129:271–9.
- Ding YK, Wu Y, Wang HD, Liu GQ, Ji WS. Effects of TNT on the thermal decomposition performance of RDX. *Explos Mater*. 2014;43:21–5.
- Zhu YL, Shan MX, Xiao ZX, Wang JS, Jiao QJ. Kinetics of thermal decomposition of  $\epsilon$ -hexanitrohexaazaisowurtzitane by TG–DSC–MS–FTIR. *J Chem Eng*. 2015;32:1164–9.
- Zhang H, Zan LJ, Zhao B, Qiu HD. Study on the thermal sensitivity of energetic materials characterized by accelerating rate calorimeter (ARC). *Appl Mech Mater*. 2013;394:45–9.
- Liu R, Zhang TL, Yang L, Zhou ZN, Hu XC. Research on thermal decomposition of trinitrophenylglucitol salts by DSC, TG and DVST. *Cent Eur J Chem*. 2013;11:774–81.
- Abd-Elghany M, Elbeih A, Hassanein S. Thermal behavior and decomposition kinetics of RDX and RDX/HTPB composition using various techniques and methods. *Eur J Energ Mater*. 2016;13:714–35.
- Elbeih A, Abd-Elghany M, Elshenawy T. Application of vacuum stability test to determine thermal decomposition kinetics of nitramines bonded by polyurethane matrix. *Acta Astronaut*. 2017;132:124–30.
- Chovancová M, Zeman S. Study of initiation reactivity of some plastic explosives by vacuum stability test and non-isothermal differential thermal analysis. *Thermochim Acta*. 2007;460:67–76.
- Shi XB, Pang WQ, Liu Q, Yang L. Studies on thermal behavior of Poly-5-vinyltetrazole and its compatibility with energetic components. *Chem Propell Polym Mater*. 2011;9:89–92.
- Delpuech A, Cherville J. Relation entre la structure électronique et la sensibilité au choc des explosifs secondaires nitrés. III. Influence de l'environnement cristallin. *Propell Explos Pyrotech*. 1979;4:61–5.
- Benchabane M. The discontinuous vacuum stability test (DVST). *J Energ Mater*. 1993;11:89–99.
- McKenney Jr MR, Stevens WE, Goguen PW. Modified vacuum thermal stability test apparatus for energetic materials. *J Energ Mater*. 2000;18:139–61.
- Egorshv VY, Sinditskii VP, Smirnov SP. A comparative study on two explosive acetone peroxides. *Thermochim Acta*. 2013;574:154–61.
- Nedel'ko VV, Korsunskii BL, Larikova TS, Chapyshev SV, Chukanov NV, Yuantsze S. Thermal decomposition of 2,4,6-triazido-1,3,5-triazine. *Russ J Phys Chem B*. 2016;10:570–5.
- Kučera V, Vetlický B. Investigation of the decomposition processes in single-base propellants under vacuum using a mini-computer-controlled automated apparatus. *Propell Explos Pyrotech*. 1985;10:65–8.
- Liu R, Zhou ZN, Yin YL, Yang L, Zhang TL. Dynamic vacuum stability test method and investigation on vacuum thermal decomposition of HMX and CL-20. *Thermochim Acta*. 2012;537:13–9.
- Zhang TL, Hu XC, Yang L, Li KY, Zhang JG, Wang WL, Wang LQ. Study on dynamic vacuum stability test (DVST) method (I). *Chin J Energ Mater*. 2009;17:549–53.
- Liu R, Yin YL, Zhang TL, Yang L, Zhang JG, Zhou ZN, Qiao XJ, Wang WJ, Wang LQ. Dynamic vacuum stability test method for thermal decomposition of CL-20. *Chin J Explos Propell*. 2011;34:21–5.
- Xiao YY, Jin B, Peng RF, Zhang QC, Liu QQ, Chu SJ, Guo ZC. Thermal decomposition of CL-20 via a self-modified dynamic vacuum stability test. *J Therm Anal Calorim*. 2017;128:1833–40.
- Luo LQ, Jin B, Xiao YY, Zhang QC, Chai ZH, Huang Q, Chu SJ, Peng RF. Study on the isothermal decomposition kinetics and mechanism of nitrocellulose. *Polym Test*. 2019;75:337–43.
- Liu R. Dynamic pressure-measuring thermal analysis technique and applications. Beijing: Beijing Institute of Technology; 2015. p. 60–6.
- Chu SJ. Thermal analysis of explosives. 1st ed. Beijing: Science Press; 1994.
- Vyazovkin S, Wight CA. Model-free and model-fitting approaches to kinetic analysis of isothermal and nonisothermal data. *Thermochim Acta*. 1999;340–341:53–68.
- Chrissafis K. Kinetics of thermal degradation of polymers. *J Therm Anal Calorim*. 2009;95:273–83.
- Hu RZ, Gao SL, Zhao FQ, Shi QZ, Zhang TL, Zhang JJ. Thermal analysis kinetics. 2nd ed. Beijing: Science Press; 2008.

**Publisher's Note** Springer Nature remains neutral with regard to jurisdictional claims in published maps and institutional affiliations.